Rain driven by receding ice sheets as a cause of past climate change

Ian Eisenman,[1,2] Cecilia M. Bitz,[2] and Eli Tziperman[3,4]

[1] The Younger Dryas cold period, which interrupted the transition from the last ice age to modern conditions in Greenland, is one of the most dramatic incidents of abrupt climate change reconstructed from paleoclimate proxy records. Changes in the Atlantic Ocean overturning circulation in response to freshwater fluxes from melting ice are frequently invoked to explain this and other past climate changes. Here we propose an alternative mechanism in which the receding glacial ice sheets cause the atmospheric circulation to enter a regime with greater net precipitation in the North Atlantic region. This leads to a significant reduction in ocean overturning circulation, causing an increase in sea ice extent and hence colder temperatures. Positive feedbacks associated with sea ice amplify the cooling. We support the proposed mechanism with the results of a state-of-the-art global climate model. Our results suggest that the atmospheric precipitation response to receding glacial ice sheets could have contributed to the Younger Dryas cooling, as well as to other past climate changes involving the ocean overturning circulation.

Citation: Eisenman, I., C. M. Bitz, and E. Tziperman (2009), Rain driven by receding ice sheets as a cause of past climate change, *Paleoceanography*, *24*, PA4209, doi:10.1029/2009PA001778.

1. Introduction

[2] As the glacial ice sheets receded 20,000–7000 years ago, the transition from ice age to modern conditions in Greenland was interrupted by a cold period between 12,800 and 11,500 years ago known as the Younger Dryas [*Alley*, 2000]. The prevailing theory for the Younger Dryas since the 1980s has been that the overflow of Lake Agassiz, a large glacial meltwater lake at the southern margin of the Laurentide Ice Sheet in North America, was diverted by the receding ice sheet between drainage routes to the Gulf of Mexico and the North Atlantic [*Rooth*, 1982; *Broecker et al.*, 1988]. This flux of freshwater into the North Atlantic is thought to have caused the density of the cold surface waters to decrease, leading to a reduction in North Atlantic Deep Water (NADW) formation and the northward transport of warmer water that feeds it [*Broecker et al.*, 1985]. Indeed, proxy reconstructions suggest that NADW formation diminished during the Younger Dryas [*Boyle and Keigwin*, 1987; *McManus et al.*, 2004], and simulations with global climate models (GCMs) have demonstrated that an imposed 0.1 Sv flux of freshwater into the 50°N–70°N Atlantic Ocean can cause widespread cooling in qualitative agreement with reconstructions from proxy records [*Manabe and Stouffer*, 1997; *Stouffer et al.*, 2006].

[3] A number of recent studies, however, have yielded results incompatible with a Younger Dryas meltwater flood. While smaller Lake Agassiz floods left vast canyons and boulder fields in today's landscape, no visible evidence has been found for flood channels associated with Lake Agassiz runoff through an eastern outlet during the Younger Dryas [*Lowell et al.*, 2005; *Teller et al.*, 2005; *Broecker*, 2006]. Furthermore, proxy reconstructions of salinity in the Gulf of St. Lawrence suggest no major change at the time of the Younger Dryas [*DeVernal et al.*, 1996], although there is conflicting proxy evidence regarding the possibility of increased meltwater runoff in this region during the Younger Dryas [*Carlson et al.*, 2007; *Broecker*, 2006].

[4] Hence the theory that the Younger Dryas was triggered by an increased freshwater flux into the North Atlantic seems to agree with proxy reconstructions and model simulations, but the source of freshwater remains elusive. The shortcomings of the Agassiz flood explanation have spurred a number of recent alternative theories that do not involve a freshwater flux into the North Atlantic Ocean, including speculations that the Younger Dryas may have been caused by a tropically driven shift in the direction of North Atlantic winds [*Seager and Battisti*, 2007], by the tropical Pacific mechanism that gives rise to the El Niño–La Niña variability [*Clement et al.*, 2001], by the atmosphere switching between multiple wind field states in the presence of glacial ice sheets [*Farrell and Ioannou*, 2003; *Wunsch*, 2006], by glacial meltwater discharge into the Arctic Ocean [*Tarasov and Peltier*, 2005], or by an extraterrestrial impact [*Firestone et al.*, 2007]. In contrast with these recent theories, we suggest an alternative North Atlantic freshwater source associated with the deglaciating Laurentide Ice Sheet. Net precipitation into the northern North Atlantic today causes a freshwater flux which is two to three times larger than the 0.1 Sv flux hypothesized to have occurred from an Agassiz flood [e.g., *Schmitt et al.*,

[1]Division of Geological and Planetary Sciences, California Institute of Technology, Pasadena, California, USA.
[2]Department of Atmospheric Sciences, University of Washington, Seattle, Washington, USA.
[3]Department of Earth and Planetary Sciences, Harvard University, Cambridge, Massachusetts, USA.
[4]School of Engineering and Applied Sciences, Harvard University, Cambridge, Massachusetts, USA.
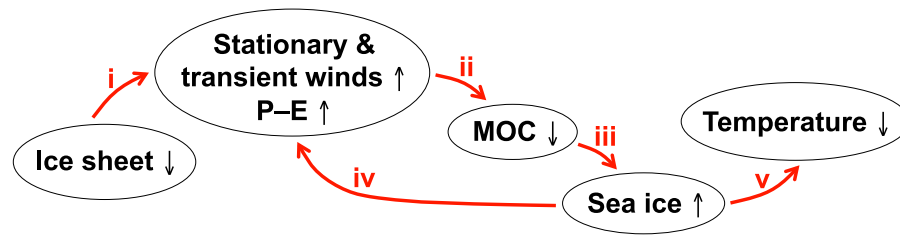
Figure 1. Schematic of the proposed mechanism. A reduction in the ice sheet size changes the surface orography and albedo, causing more northward mean winds and more intense transient eddy activity in the northern North Atlantic region (step i). These both contribute to increased northward water vapor transport and freshwater flux into the northern North Atlantic Ocean, which causes a reduction in ocean meridional overturning circulation (step ii), leading to increased sea ice cover (step iii). The sea ice causes a further increase in atmospheric eddy activity and affects the meridional specific humidity gradient, both of which are positive feedbacks which amplify the response (step iv). The extended sea ice cover causes widespread cooling in a vast region of the Northern Hemisphere (step v).

1989], so a relatively minor change in net precipitation could have a significant effect [cf. *Boyle and Keigwin*, 1987].

[5] In addition to the Younger Dryas, changes in the Atlantic Ocean overturning circulation in response to freshwater flux from melting ice are frequently invoked to explain other past climate changes. Examples include theories proposed for the Dansgaard-Oeschger abrupt warming events during the last glacial period [e.g., *Broecker et al.*, 1990] and the 100,000-year glacial cycles [e.g., *Broecker and Denton*, 1989].

[6] Here we propose a mechanism, supported by a state-of-the-art coupled GCM, by which changes in the Laurentide Ice Sheet can affect the Atlantic Ocean overturning circulation by altering the atmospheric hydrological cycle. Applying this to the Younger Dryas, we suggest that a rainy atmospheric response to the receding Laurentide Ice Sheet could have contributed to the freshwater flux that initiated the Younger Dryas cold period. The mechanism is illustrated schematically in Figure 1. In response to the changing orographic and albedo forcing of the ice sheet, the stationary wind field becomes more northward in the northern North Atlantic in tandem with an increase in transient eddy activity associated with a northward shifted jet (step i). This leads to enhanced northward moisture transport when the ice sheet size is reduced, increasing the net precipitation over the northern North Atlantic. The ocean meridional overturning circulation (MOC) weakens in response (step ii), leading to reduced northward ocean heat transport and hence extended sea ice (step iii). The sea ice in turn affects the atmospheric moisture transport to further increase net precipitation, leading to a positive feedback which reinforces the response to the change in ice sheet size (step iv). Finally, the extended sea ice expansion causes the North Atlantic cooling (step v) observed in the Greenland ice cores and other proxy records.

2. Model Description

[7] We support the proposed mechanism with simulations carried out with the National Center for Atmospheric

Research (NCAR) Community Climate System Model Version 3 (CCSM3), a coupled atmosphere–ocean–sea ice GCM [*Collins et al.*, 2006a] which we run with T31 spectral truncation in the atmosphere and an ocean grid resolution of 0.9°–3.6°. The setup of each simulation is described in detail in Appendix A. Here we summarize the main features.

[8] Large glacial ice sheets are specified in the model and then lowered in two discrete steps. Applying the proposed mechanism to the Younger Dryas, the corresponding three coupled simulations can be interpreted as corresponding to the climate system before ("LARGE" simulation hereafter), during ("MEDIUM"), and after ("SMALL") the Younger Dryas cold period. The simulations are meant to assess the plausibility of the proposed mechanism, and we impose large changes in the ice sheet forcing, equivalent to the full glacial to interglacial range. Because the purpose of these simulations is to extract dynamical insights from a comparison of three self-consistent states, we examine the climate state in each of the three simulations after it has reached approximate equilibrium with the ice sheet forcing. We do not impose any meltwater forcing associated with the receding ice sheets.

[9] To quantify the strength of the coupled climate feedbacks, we also carry out two simulations with the stand-alone atmosphere-only component of CCSM3 [*Collins et al.*, 2006b]. The sea surface temperature and sea ice cover in both atmosphere-only simulations is specified from the seasonal cycle in the LARGE coupled simulation, but one atmosphere-only simulation ("LARGE-atm") is forced by the ice sheets from the LARGE coupled simulation, while the other atmosphere-only simulation ("MEDIUMatm") is forced by ice sheets from the MEDIUM coupled simulation.

[10] The robustness of the results is addressed using a pair of higher-resolution T42 coupled model simulations. One T42 simulation ("T42LARGE") has ice sheet forcing as in the LARGE simulation, and a second T42 simulation ("T42MEDIUM") has ice sheets which are
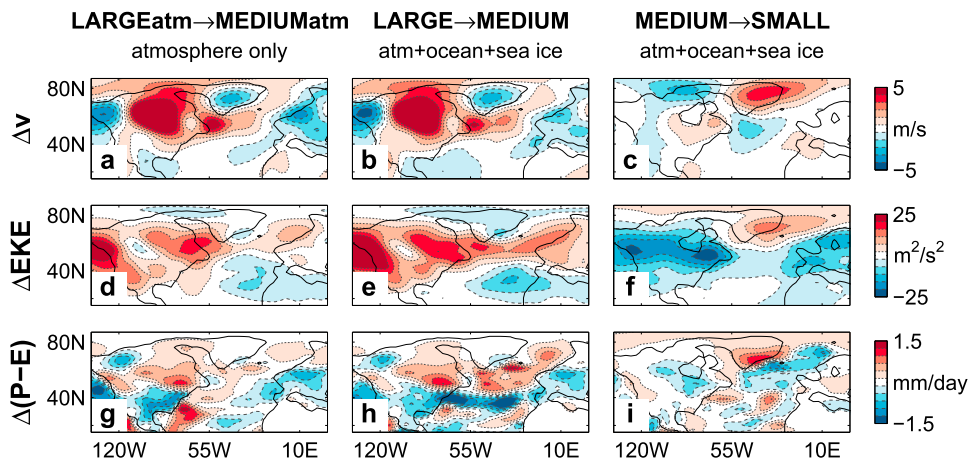
Figure 2. Annual mean change in meridional wind (Δv), eddy kinetic energy (ΔEKE), and net precipitation (precipitation minus evaporation, Δ(P-E)) associated with reducing the size of glacial ice sheets from large to medium or from medium to small. (a, d, and g) The response of the atmosphere-only GCM, with the MEDIUMatm−LARGEatm results plotted. (b, e, and h) The same fields in the coupled version from the GCM (MEDIUM−LARGE). (c, f, and i) The SMALL−MEDIUM results of the coupled GCM. The eddy kinetic energy is defined as EKE $\equiv \frac{1}{2}\overline{\mathbf{u}' \cdot \mathbf{u}'}$, where $\overline{\mathbf{u}}$ denotes the monthly mean wind velocity and $\mathbf{u}'$ denotes the departure from this mean. Meridional wind and eddy kinetic energy are averaged in pressure over the lowest 6 levels on the hybrid atmospheric grid, which approximately corresponds to the 700−1000 mb pressure range.

reduced but still somewhat larger than in the MEDIUM simulation.

3. Results

[11] In this section we examine each step of the mechanism (arrows in Figure 1) using the GCM simulations.

### 3.1. Reduced Ice Sheet Leads to More Northward Wind and Rain

[12] We begin by considering the direct effect of the receding ice sheet on the atmosphere (step i in Figure 1). We assess the atmosphere-only response to a reduction of the ice sheet size from large to medium by considering the difference between the LARGEatm and the MEDIUMatm stand-alone atmospheric model simulations. The mean winds above the ice sheet and northern North Atlantic Ocean become more northward when the ice sheet size is reduced (Figure 2a), similar to the stationary wave response expected based on idealized atmospheric models forced by varying ice sheets [Roe and Lindzen, 2001; Jackson, 2000]. The jet stream also migrates northward [cf. Li and Battisti, 2008], leading to increased vertical shear in the zonal velocity and increased transient eddy activity (Figure 2d). These changes in the mean and transient components of the wind field are both associated with more northward transport of water vapor in the atmosphere from the moist low latitudes, causing net precipitation over the northern North Atlantic to increase (Figure 2g).

[13] The annual mean surface freshwater flux into the 50°N−70°N region of the Atlantic Ocean, including continental runoff, is 0.12 Sv in the coupled LARGE simulation with a year-to-year standard deviation of 0.006 Sv during the final 20 years of the integration. In the atmosphere-only

simulations, lowering the ice sheets causes the 50°N−70°N Atlantic Ocean surface freshwater flux to increase by between 0.02 and 0.04 Sv, depending on the precise area considered (Figure 2g). About two thirds of this freshwater flux comes from runoff, and precipitation changes in the watershed region are an order of magnitude greater than evaporation changes. While this is somewhat smaller than the 0.1 Sv freshwater flux typically specified in GCM simulations of the response to massive glacial meltwater pulses, the simulated increase is largest during winter (roughly twice the annual mean value), which is when deepwater formation is most vigorous.

3.2. Rain Leads to Weakened MOC and Extended Sea Ice

[14] In the fully coupled MEDIUM simulation, there is a substantial MOC reduction associated with the change in net precipitation (Figures 3a and 3b and step ii in Figure 1). Note that changes in the atmosphere-ocean heat flux and wind stress forcing may also effect the reduction in MOC. Ocean heat flux convergence into the 40°N−80°N Atlantic Ocean is reduced by 0.2 petawatt compared with the LARGE simulation. At the same time, the stationary and eddy wind fields (Figures 2b and 2e) transport an increased amount of heat into the northern North Atlantic region (in contrast with the suggestion of Seager and Battisti [2007]), but this is more than compensated by the reduced ocean heat flux convergence. The sea ice thickness is more sensitive to changes in flux convergence in the ocean than in the atmosphere both because a substantial fraction of the atmospheric heat flux convergence is radiated upward to space [Thorndike, 1992; Cheng et al., 2007] and because much of the seasonal thickness change occurs at the base of the ice, which is insulated from the atmosphere. Hence in
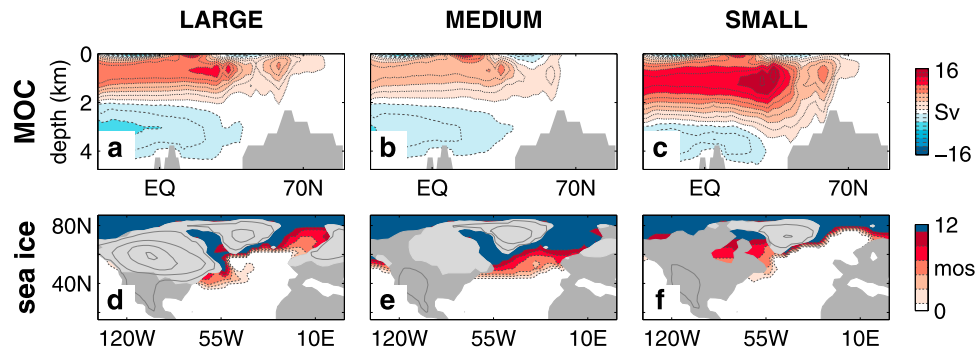
Figure 3. (a, b, and c) Annual mean MOC by Eulerian mean flow in the Atlantic basin. Red indicates clockwise circulation, and blue indicates counterclockwise circulation. Contour lines are drawn at 2 Sv intervals. Note that the secondary region of downwelling near 50°N is a typical feature of CCSM3 [*Bryan et al.*, 2006]. (d, e, and f) Number of months with sea ice filling at least 50% of each model grid box. The land area (dark gray) and glacial ice sheets (light gray) are also indicated, with surface topography contours drawn at 1 km intervals.

winter an increase in atmospheric heat flux convergence leads to an increase in ice surface temperature and upward longwave radiation, in addition to inhibiting basal growth through reduced upward diffusion of heat within the ice, whereas all of the energy from an increase in ocean heat flux convergence in an ice-covered column goes into inhibiting basal growth. In addition, the increased net precipitation in the MEDIUM simulation enhances the ocean halocline which promotes sea ice formation. As a result, North Atlantic sea ice cover extends substantially in the MEDIUM simulation (Figures 3d and 3e and step iii in Figure 1).

3.3. Positive Sea Ice Feedbacks Amplify Response

[15] The ocean and sea ice feedbacks (step iv in Figure 1) can be assessed by comparing the atmospheric fields in the atmosphere-only response to lowering the ice sheet (Figures 2a, 2d, and 2g) with the same fields in the coupled model response (Figures 2b, 2e, and 2h). While there is little change in the mean winds (Figures 2a and 2b), the jet location is displaced further northward and there is a significant enhancement of the eddy activity in the coupled simulation (compare Figure 2d with Figure 2e). Furthermore, the extended sea ice cover in the coupled MEDIUM simulation is associated with a change in the specific humidity gradient, which causes the stationary and transient wind fields to both advect increased water vapor into the northern North Atlantic (section 3.5). This leads to a further

increase in net precipitation (compare Figure 2g with Figure 2h), demonstrating that the ocean and sea ice response represents a positive feedback. This increase in net precipitation in response to an increase in northern North Atlantic Ocean surface freshwater flux also occurs in GCM simulations of the response to imposed glacial meltwater pulses [*Stouffer et al.*, 2006].

3.4. Extended Sea Ice Leads to Atmospheric Cooling

[16] The temperature change caused by reducing the ice sheets from large to medium in the coupled model (step v in Figure 1) is plotted in Figure 4b. There is widespread cooling in much of the 40°N–90°N latitude band. Because sea ice impedes heat exchange between the cold atmosphere and relatively warm ocean, it has a significant effect on air temperature [*Li et al.*, 2005], and the cooling occurs most prominently over regions where the sea ice cover has expanded (compare Figures 3d and 3e with Figure 4b). Note that there is also regional warming in Figure 4b due to the reduction in surface height and albedo over the Laurentide and Fennoscandian ice sheets, which occurs similarly in the atmosphere-only response to the lowering of the ice sheets (Figure 4a). In the coupled response, this warming signal extends over the ocean eastward of the southern part of the Laurentide Ice Sheet and is also associated with diminished sea ice cover in a region of the western North Atlantic.
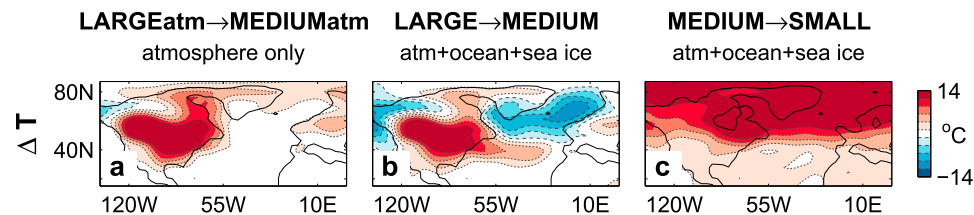
Figure 4. (a, b, and c) Annual mean change in surface air temperature associated with reducing the ice sheet size. The simulated Younger Dryas cooling (Figure 4c) in the vicinity of Greenland Summit (34°W–49°W, 69°N–76°N) is 3°C, but nearby temperatures change by over 10°C, which is a magnitude consistent with ice core reconstructions. Labels are as in Figure 2.
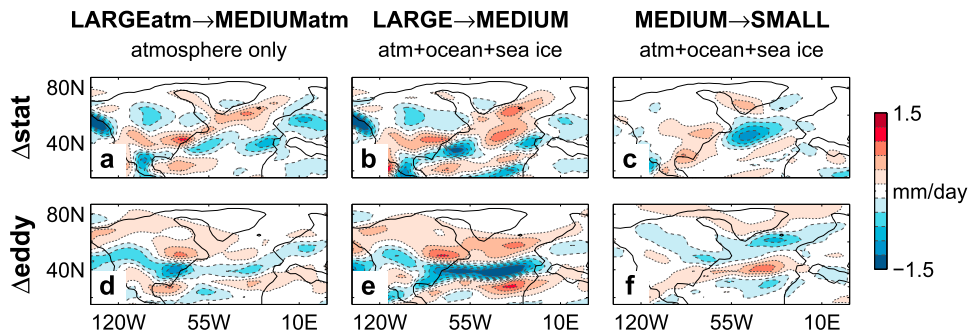
Figure 5. Column-averaged (a, b, c) stationary meridional advection and (d, e, f) transient eddy meridional flux convergence contributions to the simulated changes in annual mean net precipitation ($\Delta(P - E)$). Labels are as in Figure 2.

3.5. Atmospheric Water Vapor Budget

[17] The contributions to net precipitation can be written, in steady state, as

$$[P - E] = - \left[\left\langle \overline{u}\partial\overline{q}/\partial x + \overline{v}\partial\overline{q}/\partial y + \overline{\omega}\partial\overline{q}/\partial p + \partial(\overline{u'q'})/\partial x \right. \right.$$
$$\left. \left. + \partial(\overline{v'q'})/\partial y \right\rangle \right],$$

which is an expression of the conservation of water. Here q is specific humidity, (u, v) are (zonal, meridional) velocity, (x, y) are (zonal, meridional) displacement, ω is the vertical velocity in pressure coordinates, p is pressure, $[f]$ indicates an annual average, $\langle f \rangle$ indicates an integral in pressure over the entire column, $\overline{f}$ indicates monthly mean values, and f' indicates departures from the monthly mean. The five terms on the right-hand side of the equation represent (1) zonal, (2) meridional, and (3) convective stationary advection and (4) zonal and (5) meridional eddy flux convergence.

[18] Figure 5 shows the simulated values of the second and fifth terms, which are the dominant terms contributing to the change in $[P - E]$ in the northern North Atlantic. The stationary advection difference is larger in the coupled simulations (Figure 5b) than in the atmosphere-only simulations (Figure 5a), despite the meridional winds being similar (Figures 2a and 2b). This is consistent with the extended sea ice causing an enhanced meridional humidity gradient in the northern North Atlantic, thereby causing northward winds to advect more water vapor in the coupled simulations. Comparison of Figure 5b with Figure 5e shows that stationary advection and eddy flux convergence both contribute with similar magnitude to the simulated increase in surface freshwater flux in the coupled simulations.

## 3.6. Robustness to Model Resolution and Ice Sheet Forcing

[19] In order to address how robust our results are to model resolution and ice sheet forcing, we include a pair of higher-resolution simulations with T42 spectral truncation (see details in Appendix A3). While the T42LARGE and T42MEDIUM simulations cannot be integrated to steady state due to their computational cost and high level of long-term variability, their transient behavior supports the

mechanism presented here. The occurrence of this mechanism for more than a century at the beginning of the higher-resolution simulations, although it does not appear to be occurring on longer timescales (see Appendix A4), gives confidence that the qualitative features of the simulation results presented here are not likely to be an artifact of the atmospheric model resolution.

[20] Figures 6a, 6b, and 6c represent the higher-resolution equivalent of the results shown in Figures 2b, 2e, and 2h. Figure 6d is the higher-resolution equivalent of Figure 4b. A
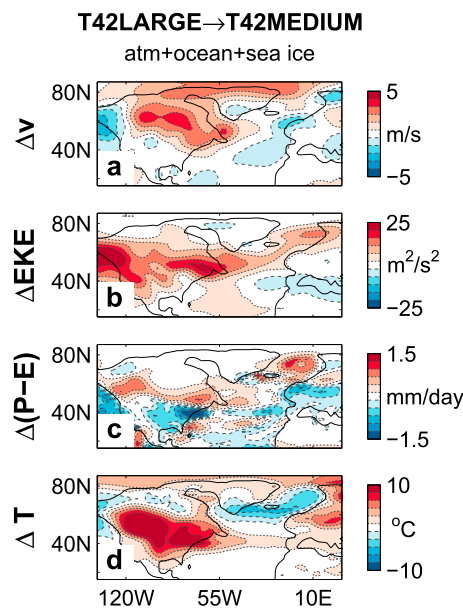
Figure 6. Results of a smaller reduction in ice sheet size specified in a higher-resolution version of the coupled model. Each plot shows T42MEDIUM − T42LARGE simulated differences. The (a) stationary and (b) transient wind responses are similar to Figures 2b and 2e, and (c) the resulting change in net precipitation is similar to Figure 2h, although the amplitudes of the responses are somewhat reduced here. (d) The northern North Atlantic cooling shows similar structure to the cooling in Figure 4b but is diminished. Note that the color range in Figure 4d indicates a smaller temperature change than in Figure 4b.
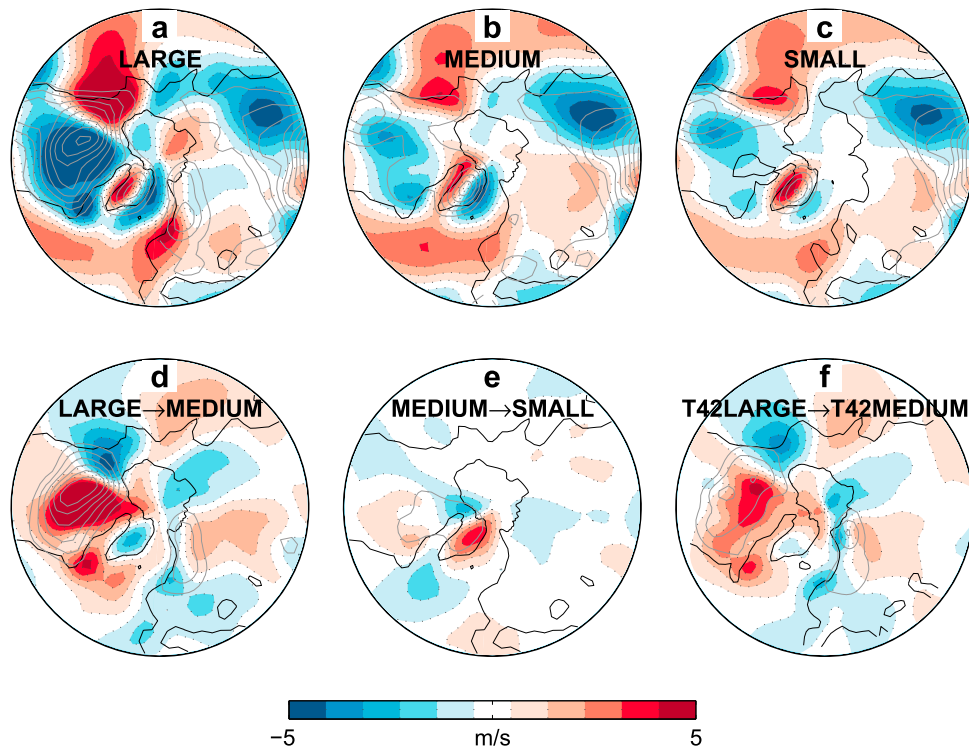
Figure 7. Polar stereographic view of the meridional wind in the lower atmosphere. The atmospheric stationary wave response to orographic forcing from the Laurentide Ice Sheet and the Rocky Mountains is fairly similar in the (a) LARGE, (b) MEDIUM, and (c) SMALL simulations; for example, there are southward winds over much of North America and northward winds over much of the North Atlantic. The wave pattern weakens and shifts slightly, however, in response to each reduction in the ice sheet height, which causes the meridional wind in the region south of Greenland to first (d) become more northward and then (e) become more southward. (f) The higher-resolution simulations show a fairly similar but somewhat weaker and westward shifted North Atlantic response. As in Figure 2, the meridional wind is averaged in pressure over the lowest 6 atmospheric levels (approximately 700–1000 mb). Surface topography (Figures 7a, 7b, and 7c) and topography differences (Figures 7d, 7e, and 7f) are indicated by gray contour lines drawn at 0.5 km intervals.

comparison of these plots demonstrates that the mean winds, atmospheric eddy activity, net freshwater forcing, and surface temperature behave in a manner that is qualitatively similar between the two resolutions. The amplitude of the changes, however, are diminished in the higher-resolution simulations, which are forced by a smaller ice sheet change.

3.7. Effect of Further Ice Sheet Reduction

[21] We find that the relationship between northern North Atlantic temperature and ice sheet size is not monotonic. When the ice sheet is reduced in the model from medium to small, northern North Atlantic mean winds become more southward (Figure 2c) and eddies weaken (Figure 2f), which both lead to a reduction in net precipitation in the northern North Atlantic (Figures 5c and 5f). This is associated with a reduction in the total freshwater flux into the northern North Atlantic (Figure 2i), more NADW formation, a more vigorous MOC (Figure 3c), contracted sea ice cover (Figure 3f), and warmer temperatures everywhere (Figure 4c). Hence our simulations suggest that a steadily receding glacial ice sheet can cause the North Atlantic region initially to cool and then to warm.

[22] The cause of this shift in sign appears to relate to the details of the ice sheet changes. Broadly speaking, the westerly mean winds are deflected northward when forced by an uphill topographic slope and deflected southward when forced by a downhill topographic slope, which excites planetary-scale stationary Rossby waves (Figures 7a, 7b, and 7c). But the changing spatial pattern of the deglaciation causes shifts in the phase and structure of the atmospheric stationary wave response. In some locations, such as the North Atlantic region south of Greenland, this mixture of weakening and shifting leads to a change in sign between the responses to the two ice sheet reductions (Figures 7d and 7e).

[23] In the T42 simulations, the change in specified ice sheet size is smaller and also somewhat spatially shifted (gray contour lines in Figures 7d and 7f). The change in meridional winds, in turn, is also reduced and slightly shifted (colors in Figures 7d and 7f). This suggests that the reduced level of cooling in the T42 simulations (Figures 4b and 6d) may be largely attributable to the differences in ice sheet forcing changes.

(a) DJF (b) JJA

-20 ΔT ($^{\circ}$C) 20
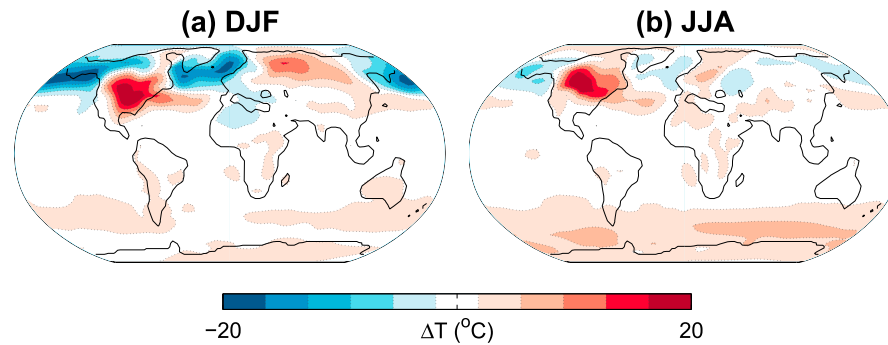
Figure 8. (a) December to February and (b) June to August surface air temperature responses to glacial ice sheets being reduced from large to medium (MEDIUM−LARGE simulation differences).

[24] The dependence of the meridional wind field on the details of the ice sheet structure, illustrated in Figure 7, suggests that cooling in the northern North Atlantic in response to a reduction in the size of glacial ice sheets may not always be expected to occur during deglaciation.

4. Discussion
4.1. Comparison With Proxy Reconstructions

[25] While this study presents sensitivity studies rather than a direct simulation of the climate during the Younger Dryas, we support the application of the proposed mechanism to the Younger Dryas cooling by comparing the results of the MEDIUM−LARGE simulation differences with proxy reconstructions of changes associated with the initiation of the Younger Dryas cold period.

[26] The broad spatial features of the cooling (Figure 4b) are approximately consistent in most regions with a temperature reconstruction map based on pollen and ice core proxy records [*Peteet*, 1995], although the simulated cooling does not extend as far west onto the coast of North America. Proxy reconstructions suggest that the Younger Dryas cooling in Greenland and around the North Atlantic occurred primarily in winter [*Denton et al.*, 2005], and our simulations are in qualitative agreement with this: the insulating effect of the sea ice [*Manabe and Stouffer*, 1980] causes the simulated MEDIUM−LARGE cooling to be about five times greater in winter than in summer in much of the North Atlantic region (Figure 8). The simulated annual mean cooling in the vicinity of the Greenland Summit ice cores is 3.0°C (Figure 4b), which is noticeably smaller than the ~10°C cooling at the beginning of the Younger Dryas in proxy temperature reconstructions [*Severinghaus et al.*, 1998; *Alley*, 2000], but simulated nearby temperatures cool by more than 10°C (Figure 4b) with wintertime simulated cooling reaching 18°C in the Norwegian Sea (Figure 8). It is thereby feasible that a relatively small change in the simulated sea ice distribution in the MEDIUM simulation, possibly associated with details of the ice sheet reconstruction or model physics, would have shifted this colder region to include Greenland Summit. The sea ice edge in the MEDIUM simulation migrates seasonally between the northernmost and southernmost latitudes of the British Isles in the eastern North Atlantic (Figure 3e),

which is consistent with climate proxy evidence that the Younger Dryas cooling in the British Isles was dramatic but largely confined to the winter months [*Atkinson et al.*, 1987].

[27] Despite the increase in net precipitation in the northern North Atlantic region in response to the ice sheet size being reduced from large to medium (Figure 2b), simulated annual precipitation in the vicinity of Greenland Summit is 14, 11, and 37 cm (water equivalent) in the LARGE, MEDIUM, and SMALL simulations, respectively. This is in qualitative agreement with proxy evidence for decreased Greenland snowfall during the Younger Dryas [*Alley et al.*, 1993].

[28] The mechanism presented here makes falsifiable predictions for new proxy reconstructions that may become available in the future. Here we discuss two separate predictions. First, we predict more southerly North Atlantic winds during the Younger Dryas (Figure 2b). The authors are aware of no proxy reconstruction to date that provides an estimate of North Atlantic winds during this period, but a recent study inferred North Atlantic ocean currents, and hence wind direction, during the Last Glacial Maximum from estimates of iceberg drift tracks using models and ice-rafted debris in deep-sea sediment cores [*Watkins et al.*, 2007]. If a similar study were applied to the Younger Dryas period, it could support or falsify the application of the proposed mechanism to the Younger Dryas.

[29] The second prediction relates to the meridional gradient in sea surface salinity. The proposed mechanism requires an increase in northward water vapor transport in the atmosphere, and hence a stronger meridional sea surface salinity gradient, in the northern North Atlantic Ocean during the Younger Dryas. This is in contrast to the typical expectation of a weaker sea surface salinity gradient associated with a less active hydrological cycle in a colder climate. Previous studies have reconstructed the North Atlantic sea surface salinity field during the Last Glacial Maximum [*Duplessy et al.*, 1991; *DeVernal et al.*, 2005], and a new method is currently being used to estimate the evolution of tropical Atlantic sea surface salinity during the past 20,000 years and could potentially be expanded to apply to the northern North Atlantic (P. deMenocal, personal communication, 2008). The application of our mechanism to the Younger Dryas could be supported or falsified by a reconstruction of the evolution of the sea surface
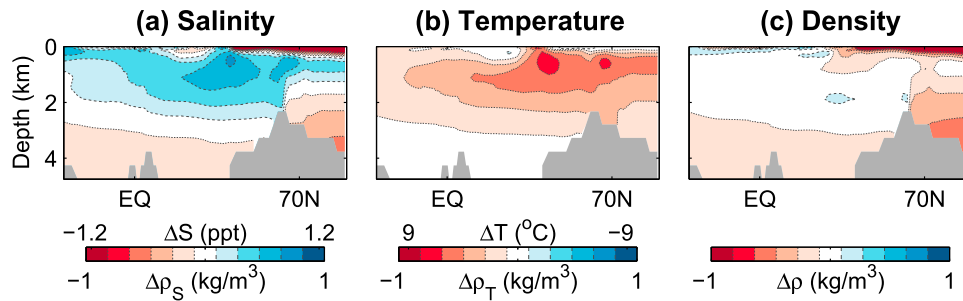
Figure 9. Vertical cross sections of the annual mean difference in temperature, salinity, and potential density in the Atlantic basin for the MEDIUM−LARGE simulated response to lowering the ice sheets. The temperature and salinity difference fields (ΔS and ΔT; indicated above color bars) have been scaled to potential density changes ($\Delta\rho$; indicated below color bars) using a linearization of the equation of state, $\Delta\rho \approx \Delta\rho_T + \Delta\rho_S$.

salinity gradient in the northern North Atlantic during the inception of the Younger Dryas.

4.2. Abruptness of Transitions

[30] Due to the computational limitations of running the GCM, we only simulate the climate response to three stationary ice sheet configurations, and in particular we do not attempt to explicitly simulate the abrupt warming that occurred at the termination of the Younger Dryas. The results are suggestive, however, of several related mechanisms by which a gradually evolving ice sheet could potentially cause a rapid change in North Atlantic climate. First, the positive sea ice feedbacks discussed above (Figures 2g and 2h) may cause nonlinear threshold behavior and switch-like warming or cooling [cf. *Gildor and Tziperman*, 2000, 2003; *Kaspi et al.*, 2004]. Second, the results depend on the location of the atmospheric jet and transient eddy field (Figure 2e), which has been suggested to be sensitive to the configuration of glacial ice sheets and possibly capable of jumping between multiple states as the ice sheet margin recedes [*Farrell and Ioannou*, 2003; *Seager and Battisti*, 2007; *Li and Battisti*, 2008]. Third, the subsurface North Atlantic Ocean in our simulations becomes both warmer and saltier in response to the ice sheet being reduced from large to medium (Figure 9), similar to what occurs in some models before a rapid MOC "flush" event [*Winton*, 1993; *Ganopolski and Rahmstorf*, 2001]. This implies the possibility that a small further reduction in the ice sheet size may lead to an abrupt, flush-like increase in the MOC. In this scenario, the warm salty subsurface North Atlantic waters are mixed to the surface and rapidly cool under contact with the atmosphere, thereby becoming dense, reducing the stability of the water column, and promoting increased MOC. These three arguments all suggest that the mechanism proposed here could cause a rapid initiation or termination of a Younger Dryas−like event in response to a small change in the gradually evolving glacial ice sheets.

5. Conclusions

[31] We have proposed a mechanism by which a rainy atmospheric response to the receding Laurentide Ice Sheet can freshen the northern North Atlantic surface ocean, weaken the Atlantic Ocean overturning circulation, and cause increased sea ice extent and widespread cooling. We suggest that this process may have provided a freshwater source that played a role in the Younger Dryas abrupt climate change event, in contrast to previous studies suggesting that the cooling was triggered by a flood of glacial meltwater.

[32] The proposed mechanism would benefit from an explicit time-dependent coupled simulation of a retreating ice sheet showing the full evolution of a cold event. Furthermore, given the sensitivity of stationary wave and eddy dynamics [*Jackson*, 2000; *Roe and Lindzen*, 2001; *Farrell and Ioannou*, 2003], the mechanism may depend on the actual shape and location of the ice sheet in addition to the total ice volume (Figure 7). Simulations with an atmospheric GCM forced by widely varying ice sheet sizes and shapes would be necessary to constrain the actual range in which a reduction of the ice sheet size leads to increased freshwater forcing and hence possibly North Atlantic cooling. The simulations presented in this study suggest that during the initiation of the Younger Dryas the glacial ice sheets may have fallen within this range.

[33] The central implication of the mechanism proposed in this study is that an evolving ice sheet can cause a change in North Atlantic net precipitation that leads to significant climate change. We emphasize that this mechanism may be relevant to climate change processes beyond the Younger Dryas in which ocean meridional overturning circulation participates, such as the Bolling Allerod, Dansgaard-Oeschger events, and Bond cycles. Similarly, a rainy response to changing ice sheet sizes and shapes could be triggered while the ice sheet grows during glaciation, in addition to during deglaciation as was emphasized here. This may affect the dynamics of glaciations and deglaciations and the possible feedback between changes in ice sheet size, North Atlantic Ocean overturning circulation, and accumulation and ablation of the ice sheets.

Appendix A: Model Description and Forcing

[34] The simulations discussed in this study are summarized in Tables A1 and A2. The coupled simulations were carried out with the NCAR CCSM3 ocean−atmosphere−

Table A1. Coupled Atmosphere–Ocean–Sea Ice Simulations[a]

Name	Resolution	Ice Sheets	Coastlines	Years	MOC
LARGE	T31	21 ka (5G), 74 m	21 ka (5G)	481–500	11.8 Sv
MEDIUM	T31	12 ka (4G), 16 m	21 ka (5G)	1070–1089	8.6 Sv
SMALL	T31	present day, 0 m	present day	414–433	16.1 Sv
T42LARGE	T42	21 ka (5G), 74 m	21 ka (5G)	380–399	16.4 Sv
T42MEDIUM	T42	14 ka (5G), 42 m	14 ka (5G)	380–399	11.2 Sv

[a]Columns are as follows: first column, simulation name; second column, model resolution; third column, paleoyear associated with the ice sheet reconstruction, whether the ICE-4G [*Peltier*, 1994] or ICE-5G [*Peltier*, 2004] reconstruction was used, and North American glacial ice sheet volume in sea level equivalent units; fourth column, paleoyear and reconstruction used for the ocean model coastlines; fifth column, simulation years used to create temporal average; and sixth column, simulated MOC strength (as defined in Figure 10 caption).

sea ice GCM [*Collins et al.*, 2006a]. The stand-alone atmospheric component of CCSM3, the Community Atmosphere Model Version 3 (CAM3) [*Collins et al.*, 2006b], was used for the atmosphere-only simulations.

A1. T31 Coupled Simulations

[35] For the main simulations discussed in this study, we use an atmospheric grid with 26 levels in the vertical and T31 spectral truncation, corresponding to a resolution of about 3.75° in latitude and longitude. The sea ice and ocean are on the "gx3v5" grid with the North Pole displaced into Greenland, which has horizontal grid spacing of roughly 0.9°–3.6° with finest resolution around Greenland [*Yeager et al.*, 2006].

[36] In the LARGE simulation, the ice sheets (specified through surface topography and land model surface type) and coastline are based on the ICE-5G reconstruction [*Peltier*, 2004] of the Last Glacial Maximum (21,000 years ago). Greenhouse gases and insolation parameters are adjusted to their approximate values 21,000 years ago (185 ppm CO_2, 350 ppb CH_4, and 200 ppb N_2O). Due to technical difficulties associated with changing the CCSM3 runoff model, the direction of runoff on land was left at the present-day configuration in all coupled simulations presented here, as has been done in previous CCSM3 paleoclimate simulations [*Otto-Bliesner et al.*, 2006a]. Note that although the introduction of the Laurentide Ice Sheet causes a considerable change in the topography over North America, the location of the continental divide remains to the west of the region with largest increases in net precipitation in Figure 2h, suggesting that the qualitative results may not be very sensitive to whether the ice sheet is accounted for in the runoff model. The ocean is initialized with conditions from the end of the higher-resolution T42LARGE simulation [*Otto-Bliesner et al.*, 2006a] described in section A3. We run the model for 500 years and discuss in this study the mean seasonal cycle from the final 20 years. The results of this simulation compare with the T42LARGE simulation approximately as would be expected based on a comparison of these two resolutions under preindustrial forcing [*Otto-Bliesner et al.*, 2006b]: the global mean surface temperature is 8.6°C, Northern Hemisphere sea ice area is 13.9 × 10^6 km², Southern Hemisphere sea ice area is 29.1 × 10^6 km², and the maximum of the Atlantic overturning stream function is 11.8 Sv at a depth of 686 m in the LARGE simulation. Note that the MOC is somewhat weaker and shallower in the LARGE simulation compared

with the SMALL simulation, with an associated enhancement in Antarctic Bottom Water. This is similar to some paleoclimate reconstructions [*Duplessy et al.*, 1980; *Curry and Lohmann*, 1982; *Lynch-Stieglitz et al.*, 1999], although results remain inconclusive [e.g., *Wunsch*, 2003]. Some coupled GCM simulations of the difference between Last Glacial Maximum and present-day climates show a similar change in MOC to what we simulate [*Shin et al.*, 2003; *Weaver et al.*, 2001], although it should be noted that other coupled GCMs simulate enhanced NADW formation under LGM forcing conditions [*Weber et al.*, 2007].

[37] The MEDIUM simulation is forced by ice sheets based on the ICE-4G reconstruction [*Peltier*, 1994] of 12,000 years ago, chosen as an intermediate point between modern and Last Glacial Maximum ice sheets. We use the ICE-4G rather than ICE-5G ice sheet reconstruction because the latter 12,000-years-ago reconstruction was not publicly available at the time the simulations were begun. To isolate the effect of the ice sheets on the atmosphere, the coastline and insolation are left identical to the LARGE simulation. Greenhouse gases are adjusted partway toward preindustrial values (233 ppm CO_2, 525 ppb CH_4, and 235 ppb N_2O). Although a separate simulation with greenhouse gas concentrations identical to the LARGE simulation was not feasible with our available computational resources, this change in greenhouse gas concentrations should be expected to cause only a small warming which would slightly reduce the large level of cooling described in this study. The implied level of warming in global mean surface temperature compared with the LARGE simulation is 0.7°C (given the 2.3°C climate sensitivity of CCSM3 at this resolution [*Kiehl et al.*, 2006]), which is far smaller than, and of opposite sign to, the 10°C simulated cooling in the northern North Atlantic. We use initial conditions from the end of the LARGE simulation, and the results discussed in this study are from the mean seasonal cycle during simulation years 1070–1089. Note that if the results of the

Table A2. Atmosphere-Only Simulations[a]

Name	Resolution	Ice Sheets	SST and Sea Ice
LARGEatm	T31	21 ka (5G), 74 m	LARGE
MEDIUMatm	T31	12 ka (4G), 16 m	LARGE

[a]Columns are as follows: first column, simulation name; second column, model resolution; third column, paleoyear, reconstruction, and volume of glacial ice sheets; and fourth column, which coupled simulation results were used to specify the SST and sea ice distribution.
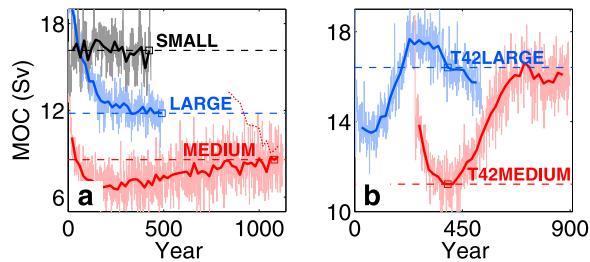
Figure 10. Time series of the strength of the North Atlantic MOC in (a) the coupled T31 simulations and (b) the higher-resolution coupled T42 simulations. The MOC strength is defined as the maximum of the annual mean stream function by Eulerian mean flow in the Atlantic basin north of 20°N and deeper than 0.5 km. Yearly values are indicated by thin lines, and thicker lines indicate 20-year averages. For each simulation, the MOC strength during the 20-year period described in this study is indicated by a square with a horizontal dashed line running through it. The dotted red line in Figure 10a shows the results of a simulation that has a warm preindustrial initial condition but is otherwise identical to the MEDIUM simulation. The red curve in Figure 10b includes both the branched Last Glacial Maximum simulation with smaller ICE-4G ice sheet forcing (years 250–290) and the T42MEDIUM simulation (years 291–898).

MEDIUM and LARGE simulations are taken literally as estimates of the climate 12,000 and 21,000 years ago, respectively, then the temperatures they produce in Greenland are in contrast with proxy records which suggest that Greenland was coldest 21,000 years ago. The LARGE and MEDIUM simulations were run on the NCAR "bluesky" cluster and took 2 months and 7 months, respectively, to complete.

[38] For the SMALL simulation, we use the results of a CCSM3 preindustrial simulation (280 ppm CO_2, 760 ppb CH_4, 270 ppb N_2O) which was previously carried out by *Otto-Bliesner et al.* [2006b] using the same T31gx3v5 model resolution. This simulation was initialized from the end of a present-day control run, and we discuss the mean seasonal cycle from the final 20 years of the 433-year simulation.

A2. T31 Atmosphere-Only Simulations

[39] To examine the atmosphere-only response to changes in the ice sheet size, we use two CAM3 simulations. In both simulations, the seasonal cycle in sea surface temperature and sea ice cover is specified from the simulated values in the LARGE coupled simulation (averaged during years 481–500). In the LARGEatm simulation, we use the land ice distribution and greenhouse gases that were specified in the LARGE simulation, whereas in the MEDIUMatm simulation the land ice and greenhouse gases are as in the MEDIUM simulation. We discuss the difference between MEDIUMatm and LARGEatm simulations (Figures 2 and 4), rather than the difference between MEDIUMatm and LARGE simulations, to minimize the effects of minor biases associated with the difference between coupled CCSM3

simulations and CAM3 simulations with the ocean and sea ice specified at their simulated CCSM3 values.

A3. T42 Coupled Simulations

[40] We include higher-resolution simulations to assess the robustness of the results. In these simulations, we use T42 spectral truncation in the atmosphere and a 0.3°–1° ("gx1v3") sea ice and ocean grid resolution.

[41] The T42LARGE simulation is a previously published Last Glacial Maximum simulation of *Otto-Bliesner et al.* [2006a], which has forcing identical to the LARGE simulation described in section A1. We use years 380–399 (Otto-Bliesner et al. describe years 250–300), although even after these additional years of integration time the simulation is still actively equilibrating (section A4).

[42] The T42MEDIUM simulation is forced by ice sheets and coastline based on the ICE-5G reconstruction of 14,000 years ago, with greenhouse gas concentrations characteristic of that time (220 ppm CO_2, 525 ppb CH_4, 235 ppb N_2O). The model initial conditions involve two steps. First, a simulation using the smaller ICE-4G Last Glacial Maximum ice sheets was branched from the T42LARGE simulation at year 250 [*Otto-Bliesner et al.*, 2006a]. Next, the T42MEDIUM simulation was branched from this reduced ice sheet run at year 290. Here we discuss the results during years 380–399, which do not appear to be near a steady state (section A4).

A4. Temporal Evolution

[43] To address the extent to which the simulations have reached a statistical steady state, the temporal evolution of the North Atlantic MOC strength for each coupled simulation is shown in Figure 10. The three T31 simulations do not show substantial trends during the final centuries of the integrations. The MEDIUM simulation shows a slight upward trend through most of the integration, but a simulation with identical forcing and a warm preindustrial initial condition (I. Eisenman et al., manuscript in preparation, 2009) (red dotted line in Figure 10) implies that the final centuries of the MEDIUM simulation may be near a statistical steady state.

[44] Both of the higher-resolution T42 simulations, in contrast, demonstrate considerable long-term variability throughout the integrations. Because of this, we discuss only the transient behavior of the T42 simulations in this study, focusing on a 20-year period near the beginning of the T42MEDIUM simulation when the difference between the two simulations is large (horizontal dashed lines in Figure 10b).

References

Alley, R. B. (2000), The Younger Dryas cold interval as viewed from central Greenland, *Quat. Sci. Rev.*, *19*(1–5), 213–226.

Alley, R. B., et al. (1993), Abrupt increase in Greenland snow accumulation at the end of the Younger Dryas event, *Nature*, *362*(6420), 527–529.

Atkinson, T. C., K. R. Briffa, and G. R. Coope (1987), Seasonal temperatures in Britain during the past 22,000 years, reconstructed using beetle remains, *Nature*, *325*(6105), 587–592.

Boyle, E. A., and L. Keigwin (1987), North Atlantic thermohaline circulation during the past 20,000 years linked to high-latitude surface temperature, *Nature*, *330*(6143), 35–40.

Broecker, W. S. (2006), Was the Younger Dryas triggered by a flood?, *Science*, *312*, 1146–1148.

Broecker, W. S., and G. H. Denton (1989), The role of ocean-atmosphere reorganizations in glacial cycles, *Geochim. Cosmochim. Acta*, *53*, 2465–2501.

Broecker, W. S., D. M. Peteet, and D. Rind (1985), Does the ocean-atmosphere system have more than one stable mode of operation?, *Nature*, *315*(6014), 21–26.

Broecker, W. S., M. Andree, W. Wolfli, H. Oeschger, G. Bonani, J. Kennett, and D. Peteet (1988), The chronology of the last deglaciation: Implications to the cause of the Younger Dryas event, *Paleoceanography*, *3*, 1–19.

Broecker, W. S., G. Bond, M. Klas, G. Bonani, and W. Wolfi (1990), A salt oscillator in the glacial Atlantic?: 1. The concept, *Paleoceanography*, *5*, 469–478.

Bryan, F. O., G. Danabasoglu, N. Nakashiki, Y. Yoshida, D. H. Kim, J. Tsutsui, and S. C. Doney (2006), Response of the North Atlantic thermohaline circulation and ventilation to increasing carbon dioxide in CCSM3, *J. Clim.*, *19*(11), 2382–2397.

Carlson, A. E., P. U. Clark, B. A. Haley, G. P. Klinkhammer, K. Simmons, E. J. Brook, and K. J. Meissner (2007), Geochemical proxies of North American freshwater routing during the Younger Dryas cold event, *Proc. Natl. Acad. Sci. U. S. A.*, *104*(16), 6556–6561.

Cheng, W., C. M. Bitz, and J. C. H. Chiang (2007), Adjustment of the global climate to an abrupt slowdown of the Atlantic meridional overturning circulation, in *Ocean Circulation: Mechanisms and Impacts, Geophys. Monogr. Ser.*, vol. 173, edited by A. Schmittner, J. Chiang, and S. Hemmings, pp. 295–313, AGU, Washington, D. C.

Clement, A. C., M. A. Cane, and R. Seager (2001), An orbitally driven tropical source for abrupt climate change, *J. Clim.*, *14*(11), 2369–2375.

Collins, W. D., et al. (2006a), The Community Climate System Model version 3 (CCSM3), *J. Clim.*, *19*(11), 2122–2143.

Collins, W. D., et al. (2006b), The formulation and atmospheric simulation of the Community Atmosphere Model version 3 (CAM3), *J. Clim.*, *19*(11), 2144–2161.

Curry, W. B., and G. P. Lohmann (1982), Carbon isotopic changes in benthic foraminifera from the western South-Atlantic: Reconstruction of glacial abyssal circulation patterns, *Quat. Res.*, *18*(2), 218–235.

Denton, G. H., R. B. Alley, G. C. Comer, and W. S. Broecker (2005), The role of seasonality in abrupt climate change, *Quat. Sci. Rev.*, *24*(10–11), 1159–1182.

DeVernal, A., C. Hillaire-Marcel, and G. Bilodeau (1996), Reduced meltwater outflow from the Laurentide ice margin during the Younger Dryas, *Nature*, *381*(6585), 774–777.

DeVernal, A., et al. (2005), Reconstruction of sea-surface conditions at middle to high latitudes of the Northern Hemisphere during the Last Glacial Maximum (LGM) based on dinoflagellate cyst assemblages, *Quat. Sci. Rev.*, *24*(7–9), 897–924.

Duplessy, J.-C., J. Moyes, and C. Pujol (1980), Deep water formation in the North Atlantic Ocean during the last ice age, *Nature*, *286*(5772), 479–482.

Duplessy, J.-C., L. Labeyrie, A. Juillet-Leclerc, F. Maitre, J. Duprat, and M. Sarnthein (1991), Surface salinity reconstruction of the North Atlantic Ocean during the Last Glacial Maximum, *Oceanol. Acta*, *14*(4), 311–324.

Farrell, B. F., and P. J. Ioannou (2003), Structural stability of turbulent jets, *J. Atmos. Sci.*, *60*(17), 2101–2118.

Firestone, R. B., et al. (2007), Evidence for an extraterrestrial impact 12,900 years ago that contributed to the megafaunal extinctions and the Younger Dryas cooling, *Proc. Natl. Acad. Sci. U. S. A.*, *104*(41), 16,016–16,021.

Ganopolski, A., and S. Rahmstorf (2001), Rapid changes of glacial climate simulated in a coupled climate model, *Nature*, *409*(6817), 153–158.

Gildor, H., and E. Tziperman (2000), Sea ice as the glacial cycles climate switch: Role of seasonal and orbital forcing, *Paleoceanography*, *15*, 605–615.

Gildor, H., and E. Tziperman (2003), Sea-ice switches and abrupt climate change, *Philos. Trans. R. Soc. London, Ser. A*, *361*(1810), 1935–1942.

Jackson, C. (2000), Sensitivity of stationary wave amplitude to regional changes in Laurentide ice sheet topography in single-layer models of the atmosphere, *J. Geophys. Res.*, *105*(D19), 24,443–24,454.

Kaspi, Y., R. Sayag, and E. Tziperman (2004), A "triple sea-ice state" mechanism for the abrupt warming and synchronous ice sheet collapses during Heinrich events, *Paleoceanography*, *19*, PA3004, doi:10.1029/2004PA001009.

Kiehl, J. T., C. A. Shields, J. J. Hack, and W. D. Collins (2006), The climate sensitivity of the Community Climate System Model version 3 (CCSM3), *J. Clim.*, *19*(11), 2584–2596.

Li, C., and D. S. Battisti (2008), Reduced Atlantic storminess during the Last Glacial Maximum: Evidence from a coupled climate model, *J. Clim.*, *21*(14), 3561–3579.

Li, C., D. S. Battisti, D. P. Schrag, and E. Tziperman (2005), Abrupt climate shifts in Greenland due to displacements of the sea ice edge, *Geophys. Res. Lett.*, *32*, L19702, doi:10.1029/2005GL023492.

Lowell, T., et al. (2005), Testing the Lake Agassiz meltwater trigger for the Younger Dryas, *Eos Trans. AGU*, *86*(40), 365–373.

Lynch-Stieglitz, J., W. B. Curry, and N. Slowey (1999), Weaker Gulf Stream in the Florida Straits during the Last Glacial Maximum, *Nature*, *402*(6762), 644–648.

Manabe, S., and R. J. Stouffer (1980), Sensitivity of a global climate model to an increase of CO_2 concentration in the atmosphere, *J. Geophys. Res.*, *85*(C10), 5529–5554.

Manabe, S., and R. J. Stouffer (1997), Coupled ocean-atmosphere model response to freshwater input: Comparison to Younger Dryas event, *Paleoceanography*, *12*, 321–336.

McManus, J. F., R. Francois, J. M. Gherardi, L. D. Keigwin, and S. Brown-Leger (2004), Collapse and rapid resumption of Atlantic meridional circulation linked to deglacial climate changes, *Nature*, *428*(6985), 834–837.

Otto-Bliesner, B. L., E. C. Brady, G. Clauzet, R. Tomas, S. Levis, and Z. Kothavala (2006a), Last Glacial Maximum and Holocene climate in CCSM3, *J. Clim.*, *19*(11), 2526–2544.

Otto-Bliesner, B. L., R. Tomas, E. C. Brady, C. Ammann, Z. Kothavala, and G. Clauzet (2006b), Climate sensitivity of moderate- and low-resolution versions of CCSM3 to preindustrial forcings, *J. Clim.*, *19*(11), 2567–2583.

Peltier, W. R. (1994), Ice age paleotopography, *Science*, *265*, 195–201.

Peltier, W. R. (2004), Global glacial isostasy and the surface of the ice-age Earth: The ICE-5G (VM2) model and GRACE, *Annu. Rev. Earth Planet. Sci.*, *32*, 111–149.

Peteet, D. (1995), Global Younger Dryas?, *Quat. Int.*, *28*, 93–104.

Roe, G. H., and R. S. Lindzen (2001), The mutual interaction between continental-scale ice sheets and atmospheric stationary waves, *J. Clim.*, *14*(7), 1450–1465.

Rooth, C. (1982), Hydrology and ocean circulation, *Prog. Oceanogr.*, *11*(2), 131–149.

Schmitt, R. W., P. S. Bogden, and C. E. Dorman (1989), Evaporation minus precipitation and density fluxes for the North Atlantic, *J. Phys. Oceanogr.*, *19*(9), 1208–1221.

Seager, R., and D. Battisti (2007), Challenges to our understanding of the general circulation: Abrupt climate change, in *The Global Circulation of the Atmosphere: Phenomena, Theory, Challenges*, edited by T. Schneider and A. H. Sobel, pp. 331–371, Princeton Univ. Press, Princeton, N. J.

Severinghaus, J. P., T. Sowers, E. J. Brook, R. B. Alley, and M. L. Bender (1998), Timing of abrupt climate change at the end of the Younger Dryas interval from thermally fractionated gases in polar ice, *Nature*, *391*(6663), 141–146.

Shin, S. I., Z. Liu, B. Otto-Bliesner, E. C. Brady, J. E. Kutzbach, and S. P. Harrison (2003), A simulation of the Last Glacial Maximum climate using the NCAR-CCSM, *Clim. Dyn.*, *20*(2–3), 127–151.

Stouffer, R. J., et al. (2006), Investigating the causes of the response of the thermohaline circulation to past and future climate changes, *J. Clim.*, *19*(8), 1365–1387.

Tarasov, L., and W. R. Peltier (2005), Arctic freshwater forcing of the Younger Dryas cold reversal, *Nature*, *435*(7042), 662–665.

Teller, J. T., M. Boyd, Z. R. Yang, P. S. G. Kor, and A. M. Fard (2005), Alternative routing of Lake Agassiz overflow during the Younger Dryas: New dates, paleotopography, and a re-evaluation, *Quat. Sci. Rev.*, *24*(16–17), 1890–1905.

Thorndike, A. S. (1992), A toy model linking atmospheric thermal radiation and sea ice growth, *J. Geophys. Res.*, *97*(C6), 9401–9410.

Watkins, S. J., B. A. Maher, and G. R. Bigg (2007), Ocean circulation at the Last Glacial Maximum: A combined modeling and magnetic proxy-based study, *Paleoceanography*, *22*, PA2204, doi:10.1029/2006PA001281.

Weaver, A. J., et al. (2001), The UVic Earth system climate model: Model description, climatology, and applications to past, present and future climates, *Atmos. Ocean*, *39*(4), 361–428.

Weber, S. L., S. S. Drijfhout, A. Abe-Ouchi, M. Crucifix, M. Eby, A. Ganopolski, S. Murakami, B. Otto-Bliesner, and W. R. Peltier (2007), The modern and glacial overturning circulation in the Atlantic Ocean in PMIP coupled model simulations, *Clim. Past*, *3*(1), 51–64.

Winton, M. (1993), Deep decoupling oscillations of the oceanic thermohaline circulation, in *Ice*

in the Climate System, *NATO ASI Ser., Ser. I*, vol. 12, edited by W. R. Peltier, pp. 417–432, Springer, Berlin.

Wunsch, C. (2003), Determining pale oceano-graphic circulations, with emphasis on the Last Glacial Maximum, *Quat. Sci. Rev.*, 22(2–4), 371–385.

Wunsch, C. (2006), Abrupt climate change: An alternative view, *Quat. Res.*, 65(2), 191–203.

Yeager, S. G., C. A. Shields, W. G. Large, and J. J. Hack (2006), The low-resolution CCSM3, *J. Clim.*, 19(11), 2545–2566.

———————————

C. M. Bitz, Department of Atmospheric Sciences, University of Washington, Seattle, WA 98195, USA.

I. Eisenman, Division of Geological and Planetary Sciences, California Institute of Technology, 1200 California Boulevard, Pasadena, CA 91125, USA. (ian@gps.caltech.edu)

E. Tziperman, Department of Earth and Planetary Sciences, Harvard University, Cambridge, MA 02138, USA.